ChemComm

Accepted Manuscript

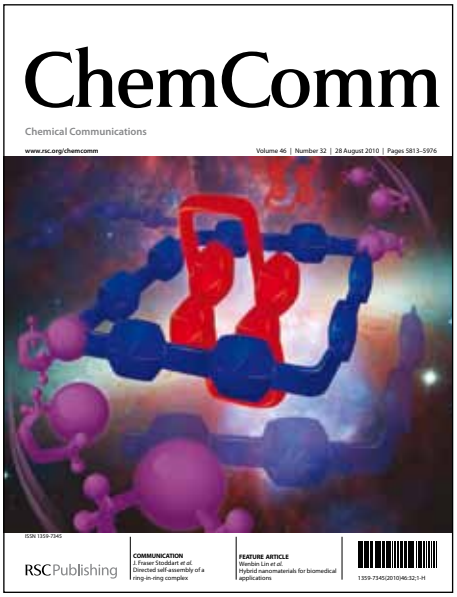

This is an *Accepted Manuscript*, which has been through the RSC Publishing peer review process and has been accepted for publication.

Accepted Manuscripts are published online shortly after acceptance, which is prior to technical editing, formatting and proof reading. This free service from RSC Publishing allows authors to make their results available to the community, in citable form, before publication of the edited article. This *Accepted Manuscript* will be replaced by the edited and formatted *Advance Article* as soon as this is available.

To cite this manuscript please use its permanent Digital Object Identifier (DOI®), which is identical for all formats of publication.

More information about *Accepted Manuscripts* can be found in the **Information for Authors**.

Please note that technical editing may introduce minor changes to the text and/or graphics contained in the manuscript submitted by the author(s) which may alter content, and that the standard **Terms & Conditions** and the **ethical guidelines** that apply to the journal are still applicable. In no event shall the RSC be held responsible for any errors or omissions in these *Accepted Manuscript* manuscripts or any consequences arising from the use of any information contained in them.

Journal Name

RSCPublishing

COMMUNICATION

A Nonlinear Approach to Surface-Enhanced Sensing in the Short-Wave Infrared

Cite this: DOI: 10.1039/xoxxoooooox

H. K. Turley,[a] J. P. Camden *[a]

Received ooth January 2012,
Accepted ooth January 2012

DOI: 10.1039/xoxxoooooox

www.rsc.org/

The surface-enhanced hyper-Raman scattering (SEHRS) of three analyte molecules has been obtained with excitation wavelengths at 1.55 and 1.8 μm. At 1.55 μm, excellent signal-to-noise ratios under modest experimental parameters demonstrate compelling potential for practical applications in chemical analysis and molecular imaging.

Excitation wavelengths in the near infrared (NIR) and short-wave infrared (SWIR) regions (0.8-2.5 μm) afford significant advantages for chemical and biological sensing applications.[1] The reduced absorption as well as reduced scattering in materials,[2] for example, supports deeper sampling depths, better contrast, and avoids problems that arise from photobleaching and photodamage. Further, wavelengths longer than 1.4 μm provide increased eye safety because these wavelengths are not focused onto the retina but are rather absorbed by the cornea and humor.[3] Despite higher water absorption, the use of SWIR wavelengths has provided unique advantages in multiphoton microscopy.[4] For example, the nonlinear excitation of molecular probes at 1.55 μm has demonstrated a three-fold improvement in penetration depth with high contrast over conventional multiphoton microscopy at 0.8 μm.[5]

Many methods of chemical analysis and imaging rely on scattering techniques, such as Raman, because of their universal applicability and nondestructive nature. Unfortunately, scattering methods utilizing SWIR excitation are limited because their sensitivity decreases as the fourth power of the excitation frequency, which leads to experimental challenges and poor limits of detection. Figure 1 overlays the water absorption bands[6] and quantum efficiency of silicon-based detector considerations. A popular SWIR excitation wavelength is 1.55 μm due to its use in the telecomm industry and in military range-finding applications.[7] The Raman fingerprint region (500 to 1500 cm^{-1}) relative to 1.55 μm excitation occurs between 1.68 and 2.02 μm. Measurement of these wavelengths commonly employs an InGaS array; however, these detectors suffer from high dark counts and are not well suited for weak scattering events. Furthermore, strong absorption bands from water overlap with and obscure the Raman fingerprint region. Despite these challenges, some success has been achieved through Fourier transform surface-enhanced Raman scattering (FT-SERS);[3,8] although, these studies required laser powers as high as 200 mW and acquisition times as long as 25 min. These extreme conditions indicate the difficulty in detecting SERS using 1.55 μm excitation.

One approach to overcoming the difficulties associated with SWIR Raman and SWIR SERS is to employ an upconversion process so that the signal can be detected in the NIR. Such an approach also confers the advantages of multiphoton imaging spectroscopies. Hyper-Raman scattering[9] is a type of nonlinear light scattering in which two photons of frequency ω scatter one photon of frequency $2\omega \pm \omega_{vib}$ where ω_{vib} corresponds to a molecular vibration. To date, the longest excitation wavelength used in hyper-Raman studies is 1.064 μm, which results in scattered wavelengths (0.54-0.58 μm) in the visible. Difficulties arise from common materials that absorb strongly in the visible such as hemoglobin and melanin, which both absorb below 0.6

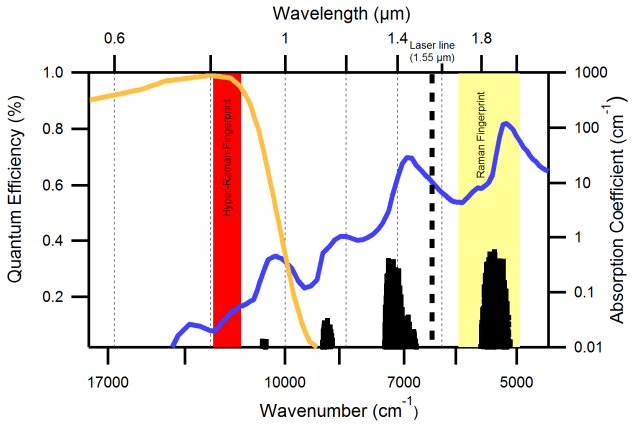

Figure 1 Absorption coefficient of liquid (blue) and atmospheric (black) water between 0.6 and 2.0 μm. The Raman (yellow) and hyper-Raman (red) fingerprint regions using 1.55 μm excitation overlay the quantum efficiency of a deep depletion CCD detector.

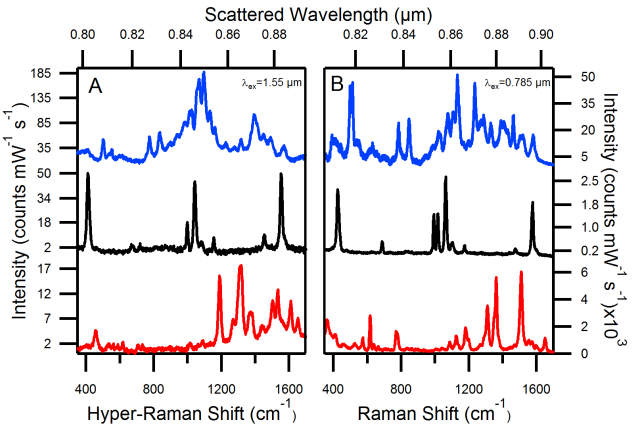

Figure 2 SEHRS (A) and SERS (B) spectra of three analyte molecules obtained using 1.55 μm and 0.785 μm excitation respectively: DTTC Iodide (blue traces), benzenethiol (black traces), and R6G (red traces). SEHRS scans were taken for 120 s at 2 mW. SERS scans were taken for 60 s at ~30 μW except for BT which was taken at ~90 μW. The spectra have been baseline corrected.

μm.[10] Additional interference from two-photon fluorescence can arise in biological samples, which typically exhibit autofluorescence below 0.7 μm. In contrast, the hyper-Raman fingerprint region relative to 1.55 μm excitation occurs in the NIR (0.80-0.88 μm), thereby, allowing the use of cost-effective silicon CCD detectors. Further, using scattered wavelengths in the NIR retains the advantages ascribed to longer wavelengths and the biological transparent region (0.7-1.1 μm).[1a]

To compensate for the weakness of the hyper-Raman effect, the signal can be increased by surface enhancement from plasmonic nanostructures. Surface-enhanced hyper-Raman scattering (SEHRS)[11] demonstrates heightened sensitivity to nanostructure-molecule interactions due to its nonlinear dependence on the excitation fields.[12] Still, the application of SEHRS is often overlooked due to its correlation with the prohibitively weak and complex hyper-Raman process; however, demonstrations of SEHRS with a low-power, mode-locked laser[13] as well as with a continuous-wave (cw) laser[14] bode well for future exploration. Recently, resonance SEHRS has even been utilized for single-molecule detection,[15] which further emphasizes the potential for high sensitivity, SEHRS based, detection.

In this report, we demonstrate that SWIR-SEHRS yields excellent sensitivity while using significantly less laser power than previous FT-SERS studies at the same wavelength. Furthermore, SEHRS detection is achieved with excitations as far red as 1.8 μm. The excitation source for hyper-Raman measurements is an optical parametric oscillator (OPO) (picoEmerald, Applied Physics & Electronics) which produces ~5 ps pulses at 80 MHz over the tunable range 0.72-0.99 μm from the signal, 1.064 μm from the pump source, and 1.15-2.03 μm from the idler. The excitation beam is directed into the back port of an inverted microscope (Nikon, Ti-U), through a 20x (Nikon, NA=0.5, air) objective. Scattered light is collected with the same objective, analyzed in a dispersive imaging spectrometer (PI Acton Research, f=0.3m), and detected with a back-illuminated deep-depletion CCD (PIXIS, Spec-10, Princeton instruments), which is operated with Winspec software (Princeton Instruments).

Colloidal nanoparticles were synthesized using the Lee and Meisel method[16] and Specifically, 400 mL of 2.6×10^{-3} M silver nitrate (Sigma-Aldrich) was brought to boil, and 100 mg of sodium citrate monohydrate (Sigma-Aldrich) was added. This solution was then boiled for ~30 minutes and diluted to 1 L after cooling. In a previous study,[15] the nanoparticles were determined to be primarily spherical and ~50 nm in diameter by TEM. The concentration of nanoparticles in the colloid solutions was estimated to be 10^{-10} M using the size and shape of the average nanoparticle. SEHRS samples were made by mixing 35 mL of the final colloid solution with Rhodamine 6G (R6G, Acros) dissolved in water to yield a final R6G concentration between 10^{-6}-10^{-10} M and aggregating with 2 mL of 1 M sodium bromide. 3,3'-Diethylthiatricarbocyanine Iodide (DTTC Iodide, Exciton) and benzenethiol (Sigma-Aldrich) were dissolved in methanol and added to the colloids after aggregation for final concentrations of 10^{-6} M and 10^{-7} M respectively.

Figure 2 displays the SEHRS spectra of R6G (10^{-6} M), benzenethiol (10^{-7} M), and DTTC Iodide (10^{-6} M) obtained with 1.55 μm excitation, and the respective SERS spectra using 0.785 μm excitation for reference. These analytes were chosen due to their varied applications. R6G is a popular analyte in single-molecule detection studies with a large, experimentally measured Raman cross section.[17] Benzenethiol is a standard probe molecule for nonresonant surface-enhanced scattering experiments. Lastly, DTTC Iodide is an effective NIR contrast agent in two-photon fluorescence microscopy[4a,5] and has an electronic resonance accessible with 1.55 μm excitation.

In all cases, the SEHRS spectra demonstrate excellent signal to noise and allow for clear identification. In the SEHRS spectrum of R6G, the location of prominent peaks around 1190, 1318, 1535, and 1610 cm^{-1} agree with previous studies.[18] When compared to spectra obtained at shorter wavelengths, however, the SEHRS spectrum exhibits differences in the relative peak intensities, which can be attributed to the lack of resonance effects. The SEHRS of benzenethiol has not been previously reported, but the prominent peaks around 424, 1022, 1068, and 1571 cm^{-1} coincide with band assignments found in the SERS spectrum. The subtle differences between the SEHRS and SERS spectra for each molecule demonstrate the complex interplay of electronic states and molecular symmetry. While a full explanation of such effects is beyond the scope of this communication, we have previously demonstrated that such assignments are possible due to the unique information encoded in SEHRS spectra.[18-19]

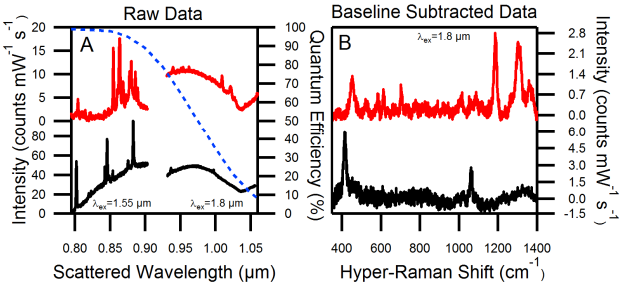

Figure 3 SEHRS spectra taken of R6G (red) and Benzenethiol (black) on Ag colloids. Panel A compares the raw data from 1.55 μm and 1.8 μm excitation with the quantum efficiency of the CCD (blue). Panel B presents baseline corrected data from 1.8 μm excitation. The scans at 1.8 μm were taken for 1 hr with 2 mW of laser power. The raw data at 1.8 μm has been corrected for the dropping CCD quantum efficiency.

In addition to 1.55 μm, we explored a range of SWIR wavelengths. Figure 3A overlays the quantum efficiency of the CCD and the raw SEHRS spectra of R6G and benzenethiol obtained at 1.55 and 1.8 μm. The spectra taken with 1.8 μm are divided by the quantum efficiency of the CCD to adjust for the drop in detector sensitivity. Despite this correction, the hyper-Raman peaks beyond 1400 cm^{-1} are lost in the background. Nevertheless, the spectra are still easily attributed to the SEHRS of the underlying analyte molecules (Figure 3B). Figure 3A reveals that long-wavelength SEHRS is limited by the capabilities of our detector, not the intrinsic weakness of the hyper-Raman effect. For comparison, the Raman shifted light from 1.8 μm excitation appears between 2.0-4.9 μm (500-3500 cm^{-1}), which overlaps common IR absorption bands and makes detection highly impractical. The hyper-Raman fingerprint region (0.94-1.05 μm), however, remains in the biological-transparent, NIR region.

Performing SEHRS studies in the SWIR region presents unique opportunities for spectroscopic sensing. Previous reports demonstrate that wavelength-scanned SEHRS studies can elucidate the two-photon properties of a visible dye molecule. With excitations in the SWIR, similar studies can now be extended to NIR chromophores. Another promising application is the use of nanotags for covert taggants and biological labeling. While SERS nanotags are commonly used at visible and NIR wavelengths,[20] our work suggests that SEHRS nanotags could be easily extended to SWIR wavelengths.

The development of simple, ultrafast fiber lasers,[21] originally designed for optical telecommunications around 1.55 μm, suggests that low-cost sensing platforms utilizing SEHRS could be constructed for industrial, biological, and military applications. For example, there are turnkey, fiber lasers capable of producing <5 ps pulses at 100 MHz around 1.55 μm that are an order of magnitude cheaper than the OPO used herein. Additionally, inexpensive, diode-based cw lasers could provide the most economical approach considering the recent demonstration of SEHRS from cw excitation.[14]

In conclusion, we have recorded SEHRS spectra from three analyte molecules using excitation wavelengths of 1.55 and 1.8 μm. Despite the considerable red-shifting of the laser from previous SEHRS studies we still obtain excellent signal-to-noise ratios and low limits of detection. When compared to conventional FT-SERS at the 1.55 μm, our method requires significantly lower laser powers and shorter acquisition times. These accomplishments bode well for the future development of plasmon-enhanced nonlinear techniques like SEHRS.

Notes and references

[a] Department of Chemistry, University of Tennessee, Knoxville, TN 37996-1600, United States. E-mail: jcamden@utk.edu

This work was supported by the University of Tennessee and the U.S. National Science Foundation under Grant CHE-1150687.

1. (a) K. König, *J. Microsc.*, 2000, **200**, 83-104; (b) E. M. Sevick-Muraca and J. C. Rasmussen, *J. Biomed. Opt.*, 2008, **13**, 041303-041303; (c) K. Welsher, S. P. Sherlock and H. J. Dai, *Proc. Natl. Acad. Sci. U. S. A.*, 2011, **108**, 8943-8948.
2. A. N. Bashkatov, E. A. Genina, V. I. Kochubey and V. V. Tuchin, *J. Phys. D Appl. Phys.*, 2005, **38**, 2543-2555.
3. H. Huang, C. Shende, A. Sengupta, F. Inscore, C. Brouillette, W. Smith and S. Farquharson, *J. Raman Spectrosc.*, 2012, **43**, 701-705.
4. (a) S. Yazdanfar, C. Joo, C. Zhan, M. Y. Berezin, W. J. Akers and S. Achilefu, *J. Biomed. Opt.*, 2010, **15**; (b) K. Murari, Y. Y. Zhang, S. P. Li, Y. P. Chen, M. J. Li and X. D. Li, *Opt. Lett.*, 2011, **36**, 1299-1301.
5. M. Y. Berezin, C. Zhan, H. Lee, C. Joo, W. J. Akers, S. Yazdanfar and S. Achilefu, *J. Phys. Chem. B*, 2011, **115**, 11530-11535.
6. (a) L. S. Rothman et al., *Quant. Spectrosc. Ra*; (b) G. M. Hale and M. R. Querry, *Appl. Opt.*, 1973, **12**, 555-563.
7. H. Haan, M. Gerken and M. Tausendfreund, *8th International Symposium on Communication Systems, Networks & Digital Signal Processing (CSNDSP)*, 2012.
8. K. A. Lynn, G. McNay, D. A. Eustace, N. C. Shand and W. E. Smith, *Analyst*, 2010, **135**, 1904-1905.
9. (a) A. M. Kelley, in *Annu. Rev. Phys. Chem.*, eds. S. R. Leone, P. S. Cremer, J. T. Groves, M. A. Johnson and G. Richmond, 2010, vol. 61, pp. 41-61; (b) L. D. Ziegler, *J. Raman Spectrosc.*, 1990, **21**, 769-779.
10. G. Zonios, J. Bykowski and N. Kollias, *J. Invest. Dermatol.*, 2001, **117**, 1452-1457.
11. (a) A. V. Baranov and Y. S. Bobovich, *JETP Letters*, 1982, **35**, 181-183; (b) D. V. Murphy, K. U. Vonraben, R. K. Chang and P. B. Dorain, *Chem. Phys. Lett.*, 1982, **85**, 43-47.
12. (a) J. T. Golab, J. R. Sprague, K. T. Carron, G. C. Schatz and R. P. Vanduyne, *J. Chem. Phys.*, 1988, **88**, 7942-7951; (b) J. Kneipp, H. Kneipp and K. Kneipp, *Proc. Natl. Acad. Sci. U. S. A.*, 2006, **103**, 17149-17153.
13. W. N. Leng and A. M. Kelley, *J. Am. Chem. Soc.*, 2006, **128**, 3492-3493.
14. T. Itoh, Y. Ozaki, H. Yoshikawa, T. Ihama and H. Masuhara, *Appl. Phys. Lett.*, 2006, **88**, 3.
15. C. B. Milojevich, B. K. Mandrell, H. K. Turley, V. Iberi, M. D. Best and J. P. Camden, *The Journal of Physical Chemistry Letters*, 2013, **4**, 3420-3423.
16. P. C. Lee and D. Meisel, *J. Phys. Chem.*, 1982, **86**, 3391-3395.
17. E. C. Le Ru and P. G. Etchegoin, in *Annu. Rev. Phys. Chem.*, eds. M. A. Johnson and T. J. Martinez, Annual Reviews, Palo Alto, 2012, vol. 63, pp. 65-87.
18. C. B. Milojevich, D. W. Silverstein, L. Jensen and J. P. Camden, *Chemphyschem*, 2011, **12**, 101-103.
19. (a) C. B. Milojevich, D. W. Silverstein, L. Jensen and J. P. Camden, *J. Am. Chem. Soc.*, 2011, **133**, 14590-14592; (b) C. B. Milojevich, D. W. Silverstein, L. Jensen and J. P. Camden, *J. Phys. Chem. C*, 2013, **117**, 3046-3054.
20. W. E. Doering, M. E. Piotti, M. J. Natan and R. G. Freeman, *Adv. Mater.*, 2007, **19**, 3100-3108.
21. D. J. Richardson, J. Nilsson and W. A. Clarkson, *J. Opt. Soc. Am. B*, 2010, **27**, B63-B92.